Self-imaging and high-beam-quality operation in multi-mode planar waveguide optical amplifiers

Howard J Baker, Jason R Lee, Denis R Hall
Department of Physics, Heriot-Watt University, Edinburgh EH14 4AS, United Kingdom
h.j.baker@hw.ac.uk

Abstract: Self-imaging in a multi-mode active waveguide is examined as a method to preserve beam quality when amplifying a fundamental gaussian beam. Misalignment tolerance, gain saturation and thermal lensing effects are evaluated for the use of self-imaging in high average power, diode-pumped, planar waveguide lasers.

OCIS codes: (140.4480) Optical amplifiers, (230.7390) Planar waveguide, (350.6830) Thermal lensing

References and Links

1. D. Pelaez-Millas, A. Faulstich, H. J. Baker and D. R. Hall, "A planar waveguide Nd:YAG laser, face pumped by laser diode bars," in *XI Int. Symp. on Gas Flow and Chemical Lasers and High Power Laser Conference, Edinburgh 1996*, H. J. Baker, ed., Proc. SPIE **3092**, 25-28 (1997).
2. H. J. Baker, A. A. Chesworth, D. Pelaez-Millas and D. R Hall, "A planar waveguide Nd:YAG laser with a hybrid waveguide-unstable resonator," Opt. Commun. **191**, 125-131 (2001).
3. J. R. Lee, H. J. Baker, G. J. Friel, G. J. Hilton and D. R. Hall "High-average-power Nd:YAG planar waveguide laser, face-pumped by 10 laser diode bars" Opt. Lett. **27**, 524-526 (2002)
4. R. J. Beach, S. C. Mitchell, H. E. Meissner, O. R. Meissner, W. K. Krupke, J. M. McMahon and W. J. Bennett "Continuous wave and passively Q-switched cladding pumped planar waveguide lasers" Opt. Lett. **26** 881-3 (2001).
5. D. P. Shepherd, S. J. Hettrick, C. Li, J. I. MacKenzie, R J. Beach, S. C. Mitchell and H. E. Meissner, "High-power planar dielectric waveguide lasers," J. Phys.D: Appl.Phys. **34**, 2420-32 (2001).
6. R. Ulrich and G. Ankele "Self-imaging in homogeneous planar optical waveguides." Appl. Phys. Lett. **27**, 337-9 (1975).
7. J. M. Heaton, R. M. Jenkins, D. R. Wright, J. T. Parker, J. C. H. Birbeck and K. P. Hilton "Novel 1-to-N way integrated optical beam splitters using symmetric mode mixing in GaAs/AlGaAs multimode waveguides." Appl. Phys. Lett. **61**, 1754-7 (1992) .
8. D. P. Shepherd, C. L. Bonner, C. T. A. Brown, W. A. Clarkson, A. C. Tropper, D. C. Hanna and H. E. Meissner, "High-numerical-aperture, contact-bonded, planar waveguides for diode-bar-pumped lasers." Opt. Commun. **160**, 47-50 (1999).
9. J. R. Lee, G. J. Friel, H. J. Baker, G. J. Hilton and D. R. Hall "A Nd:YAG planar waveguide laser operating at 121 W output with face-pumping by diode bars, and its use as a power amplifier" in *Advanced Solid-State Lasers, 2001* ed. C. Marshall, Trends in Optics and Photonics **50**, 36-40 (2001)
10. A. E. Siegman, *Lasers* (University Science Books, 1986) Chap. 7.
11. Q. Cao, H. J. Baker and D. R. Hall "Transverse mode propagation and gain coefficients in a planar waveguide CO_2 laser amplifier." IEEE J. Quant. Electron. **37** 376-383 (2001)

1. Introduction

Active planar waveguides, usually using diode pumping of rare earth doped cores, are increasingly important as small-signal optical amplifiers for telecommunications and as high average power lasers. Planar guides may be fabricated with a small core height to ensure only guiding of a fundamental mode, but the resulting small active volume means that amplified spontaneous emission, up-conversion loss, parasitic oscillation, etc, are serious limitations on the pump power which may be used. Coupling of light from pump sources such as diode laser bars is also difficult. Planar waveguide amplifying structures are length limited (< 0.06 m), and increased active volume is obtained by width scaling rather than length. For very high power lasers it is an advantage to increase the core height, to include more active material and make coupling of pump light from multiple diode laser bars more effective, at the cost of allowing multi-mode propagation in the core.

#767 - $15.00 US Received January 30, 2002; Revised March 25, 2002

We have developed Nd:YAG planar waveguide lasers which use 200 μm core height and now produce 150 W *cw* output, when pumped by 10 diode bars [1-3]. In the transverse direction, step-index guiding is produced by the small refractive index difference between the Nd:doped core and the undoped YAG cladding at diffusion-bonded interfaces. The 1 mm x 11 mm x 60 mm waveguide structure supports typically tens of transverse guided modes. On a smaller power scale, a similar structure has recently been reported for Yb:YAG with a single mode core in a cladding-pumped configuration [4,5]. In both cases, satisfactory mode control is obtained for the lateral direction by use of an unstable resonator configuration [2,5]. For operation in the power range beyond the current 150 W level, the Nd:YAG waveguide devices require resonators or MOPA configurations which will provide essentially a gaussian transverse beam output whilst using a multi-mode planar waveguide active sections.

This paper explores use of the well-known self-imaging properties of multi-mode planar waveguides [6] to conserve the beam quality from a fundamental gaussian mode source in a transit through a multi-mode planar waveguide amplifier, in the presence of input misalignment, gain saturation and thermal lens effects. One-dimensional numerical mode superposition is used to show the imaging behavior in the transverse direction of the waveguide section. To forge a link to current practice for understanding free-space laser beam propagation, the waveguide imaging calculations are followed by numerical calculation of the well-known M^2 parameter, determined from exit beam profiles using diffraction integrals, followed by second moment intensity integrals.

2. Imaging of a gaussian beam through a passive planar waveguide.

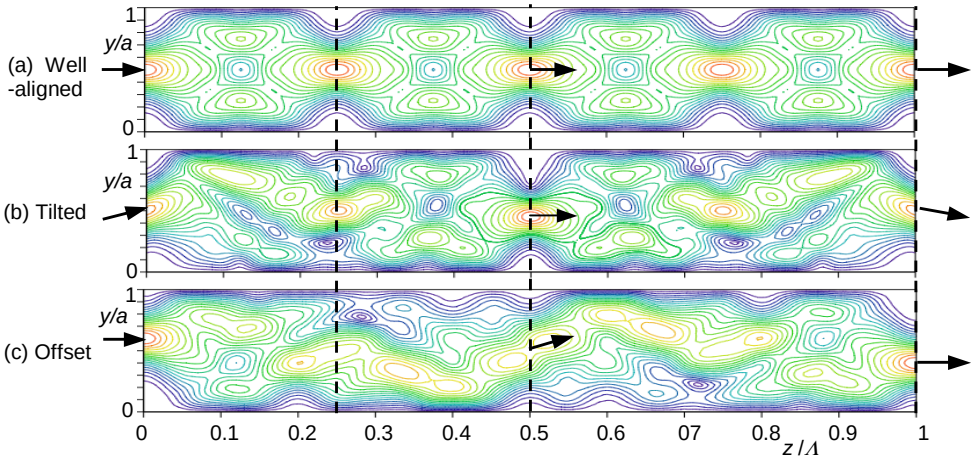

Fig. 1. Amplitude contour maps for propagation through an imaging length of waveguide, for (a) an axially aligned input gaussian beam, (b) a tilted beam and (c) an offset beam.

For a strongly guided structure with large core-cladding index difference, the core amplitude profiles are cosine or sine functions with near-zero amplitude at the core-cladding boundary. The mode propagation constant β_m, for the waveguide mode of order m is:

$$\beta_m = -\frac{\lambda \pi m^2}{4 n_1 a^2} \qquad (1)$$

The refractive index of the core is n_1 and λ is the free-space wavelength. The quadratic mode order dependence gives a characteristic distance of propagation $\Lambda = 4 n_1 a^2/\lambda$ where all modes arrive at the exit with the same phase, and the input amplitude profile is reconstructed exactly in a loss-free, straight waveguide. We refer to Λ and some of its fractions as imaging lengths of the waveguide structure. The first image occurs at $\Lambda/4$, where all the even modes arrive at the exit with the same phase, but differing to that of all the odd modes. In this case an axially symmetric input profile is needed to obtain imaging. Other fractions of Λ are used in multi-

#767 - $15.00 US
Received January 30, 2002; Revised March 25, 2002

mode 1 to N splitters in waveguide technology [7].

An undersized Gaussian beam $A(y,0)$ at the input excites a coherent superposition of guided modes with amplitudes B_m obtained by the Fourier integrals:

$$B_m = \sqrt{\frac{2}{a}} \int_0^a A(y,0) \sin\left(\frac{m\pi y}{a}\right) dy \tag{2}$$

In the case of a gaussian input beam, $A(y,0)$ may include beam curvature, tilt and offset. Using the mode-dependent phase shifts calculated from Equ. (1), the profile at distance z is:

$$A(y,z) = \sqrt{\frac{2}{a}} \sum_m B_m \exp(-j\beta_m z) \sin\left(\frac{m\pi y}{a}\right) \tag{3}$$

As an example, Fig. 1 shows amplitude contour maps for a gaussian beam input with a waist spot size $w = 0.2a$. Fig. 1(a) is for the beam axially centered, generating even modes and shows perfect imaging for all lengths that are a multiple of $\Lambda/4$. Fig. 1(b) has an external input tilt angle $\theta = \lambda/2a$ and Fig. 1(c) has an offset $\delta = 0.1\ a$. In these cases odd order modes are introduced, and imaging is perfect at only Λ where the waveguide section acts as an inverter. The $\Lambda/2$ length converts tilts to offsets and vice versa, and the imaging is aberrated. The $\Lambda/4$ length is relatively poor at imaging with these examples of input misalignment. To further quantify the alignment sensitivity of imaging, the M^2 beam propagation factor has been calculated for the beam leaving the waveguide at lengths of $\Lambda/4$, $\Lambda/2$ and Λ, shown in Fig. 2.

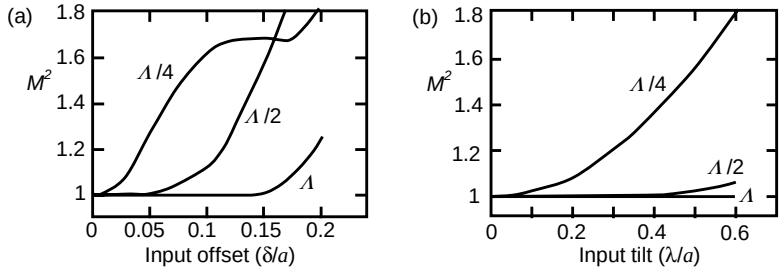

Fig. 2. Exit beam propagation factor M^2 for (a) varying input beam offset and (b) varying input beam tilt for the three waveguide lengths indicated, calculated for an input spot size $w = 0.2\ a$

Clearly the $\Lambda/4$ case has significant intolerance to the inevitable alignment errors of a practical system. In reality it is difficult to ensure that the input beam has M^2 less than 1.2 in high power systems and exit M^2 values up to 1.2 or 1.3 may still be acceptable.

The strongly guided case discussed above corresponds for example to YAG/sapphire composites [8] with a core index $n_1 = 1.82$ and cladding index $n_2 = 1.76$, giving a large number modes to image small values of the ratio w/a. For weak guiding [1-5] when the index difference is produced only by doping with $(n_2 - n_1) \sim 10^{-3}$, adjustment is needed to allow for the finite extent of cladding evanescent waves. An effective guide height $a' = a + \delta$, determined by the standard analysis method for a symmetric planar waveguide, increases the imaging length by several percent. For the 200 μm core in our Nd:YAG/YAG waveguide [1-3], the correction δ is 5.4 μm. The reduced number of guided modes is still sufficient for imaging of gaussian beams with the large w/a value in Figs. 1 and 2.

3. Gain saturation and imaging.

In Fig. 1, the multi-mode propagation excited by the gaussian input tends to fill out the waveguide, giving the opportunity for better gain saturation near the core boundaries. Here we investigate the effect by including saturable gain in the modeling. An example of the results of this procedure applied to the 200 μm core Nd:YAG laser [1-3] has been presented previously [9] and more details are given here. The method divides the imaging length into 10 sub-sections, each with a central saturable gain sheet. Equations (1)-(3) define the beam

#767 - $15.00 US Received January 30, 2002; Revised March 25, 2002

propagation between gain sheets. Gain saturation is described in the usual way [10] in terms of the intensity profiles $I(y,z)$ normalized to the saturation intensity I_s. The calculations use n_1=1.82, guide height a = 200 μm, effective height a' = 205.4 μm and 1.064 μm wavelength. The gain coefficient is set at 40 m^{-1}, giving a small signal gain of 17.8 in a single pass through the 72 mm long section. Fig. 3 shows the resulting evolution of the intensity through the $\Lambda/4$ imaging section for an axially aligned input beam waist, with $w = 0.2a$ and axial intensity $I = 2I_s$. The calculations show that the mode coupling produced by saturation is not strong enough to change the imaging mechanism significantly, and a good beam quality output is obtained. The exit beam in Fig. 3 has M^2 of 1.01 and is only slightly broadened by the saturation process, relative to the input gaussian profile.

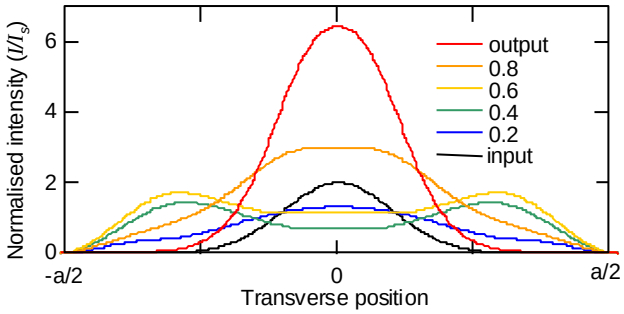

Fig. 3. Imaging of a gaussian beam during saturated amplification in an active $\Lambda/4$ waveguide.

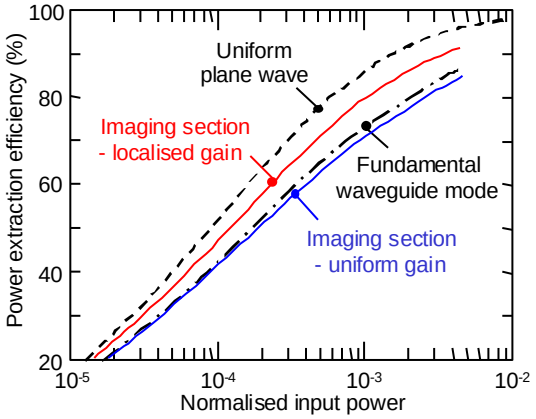

Fig. 4. Power extraction efficiency for varying input power in the saturating amplifier region. Imaging sections with uniform and partially localized gain are compared to saturation by a fundamental waveguide mode and a uniform plane wave.

The intermediate profiles in Fig. 3 show an improved fill-factor near the center of the waveguide section. This has been investigated by calculation of power extraction efficiency from the section when operating as single pass power amplifier with varying input power. As a reference, saturation by a uniform intensity wave is shown in Fig. 4, using standard formulae [10] for the fraction of the available power extracted as a function of input power which is normalized to the product $I_s.a_.$. The uniform wave gives the best extraction efficiency possible for one-way gain saturation. Using the 10 sub-section model, the same data is generated for only the fundamental waveguide mode in the core, shown as the second broken line in Fig. 4. The poorer mode-gain overlap reduces the extraction efficiency at any input power to typically 0.8 of the maximum. The efficiency calculation for the imaging condition in Fig. 3 is similar to that for the single fundamental mode, and the improved saturation uniformity in the mid-section is cancelled by the reduced beam size at the output end.

Improvement in extraction efficiency can be obtained by localizing the gain in the center

#767 - $15.00 US
Received January 30, 2002; Revised March 25, 2002

of the imaging section, as in the fourth curve in Fig. 4, where only the six central sections have gain, with a coefficient increased to preserve the overall small signal amplification. The extraction efficiency is now improved to 88% of the limiting case. This localization of pumping is possible for a 4-level gain medium such as Nd:YAG, but not for the quasi-3-level Yb:YAG material. In the latter case, a shorter active waveguide in series with undoped waveguides or short free-space sections will be necessary.

4. Thermal lens effects in active waveguides

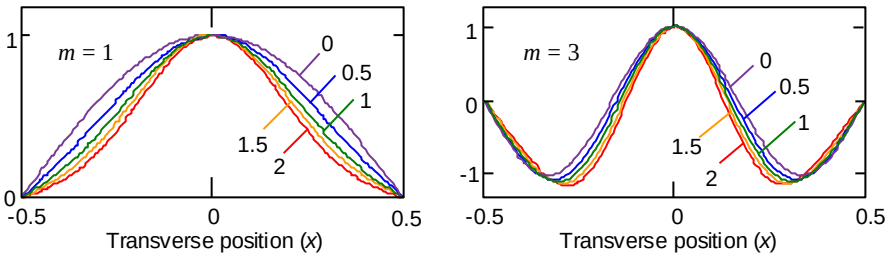

Fig. 5. Amplitude profiles for the m = 1 and m = 3 modes with the varying values of the lensing parameter ρ indicated.

In a uniformly-pumped active waveguide with a large core and double-sided cooling, as in ref. 3, the waste heat produces an axially-symmetric parabolic temperature profile and consequently a positive lens through the material dn/dT and stress-optic effects. The temperature differential is low and the material constants can be assumed constant across the core. Previously [3] we have shown that the lens does not seriously affect the fundamental waveguide mode until a specific pump power at which the thermal lens guide determines a narrower fundamental mode than the step-index guide height. In terms of the thermal power density Q dissipated in the core, an exactly parabolic variation of index in the core and a thermal conductivity κ gives:

$$Q(\max) = \frac{\pi^2 \lambda^2 \kappa}{n_1 (dn/dT) a^4} \tag{4}$$

This limit marks the onset of noticeable change in the spatial profile of the mode, as shown later. However, the thermal lens produces a change to the relative propagation constants of the modes below this power dissipation level, and hence modifies the production of images. For simplicity, the strong guiding case is investigated, without gain, allowing general conclusions to be made in terms of a normalized lensing parameter defined as $\rho = Q/Q(\max)$, the unperturbed imaging length $\Lambda = 4\, n_1 a^2/\lambda$, and the reduced transverse co-ordinate $x = y/a$. The mode equation resulting from the introduction of these parameters is:

$$\frac{d^2\psi}{dx^2} - \pi(\Lambda\beta)\psi + \rho\pi^2(1-4x^2)\psi = 0 \tag{5}$$

A numerical method is used to solve Equ. (5) with zero amplitude boundary conditions at the core edges [11], giving the eigenmodes ψ_m of the guide and their corresponding dimensionless propagation factors ($\Lambda\beta_m$). The variation of the normalized amplitude profiles of the m = 1 and m = 3 modes is shown in Fig. 5 for the lensing parameter ρ between 0 and 2. For the fundamental mode, the transition can be seen from a cosine profile at ρ = 0 to a clearly gaussian profile at ρ = 2. The higher order modes also begin to take on the appearance of Hermite-gaussian profiles but at higher values of ρ than shown. The mode propagation constants are no longer proportional to m^2 and there is not an exact imaging length where all modes in the superposition excited by the input beam arrive in phase at the output. To investigate the disturbance of the basic imaging principle covered in Sections 2 and 3, calculations of the in-guide profiles and exit beam M^2 parameter as a

#767 - $15.00 US Received January 30, 2002; Revised March 25, 2002

function of waveguide length have been carried out using the numerically determined mode profiles ψ_m and reduced propagation constants $\Lambda\beta_m$.

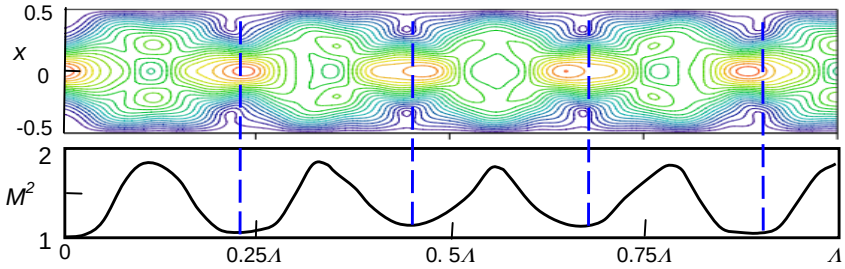

Fig. 6. Amplitude contour map for imaging in an active waveguide with a lensing parameter $\rho = 0.5$ and input beam with $w = 0.2a$. The lower curve is the M^2 beam propagation factor calculated from the sequence of beam profiles.

Fig. 6 shows an example of the calculations for a lensing parameter $\rho = 0.5$ and an input beam with $w/a = 0.2$. If Fig. 6 is compared with Fig. 1(a), it can be seen that periodic images still appear but the imaging length is shortened and the beam profile is distorted. The M^2 propagation factors at the beam waist positions indicated by the broken lines are in the range 1.05 to 1.12. Calculations over a range of the lensing parameter ρ are summarized in Fig. 7. The $\Lambda/4$ imaging length reduces progressively with lensing, and becomes determined mainly by the phase coincidence of modes $m = 1$ and $m = 3$, which carry most of the power when a gaussian beam is input on-axis. Low values of exit M^2 require a value of w/a that just under-fills the waveguide. Clearly, optical designs using the gaussian self-imaging property become dependent on the pump power when the limiting dissipation given by Equ. (4) is used.

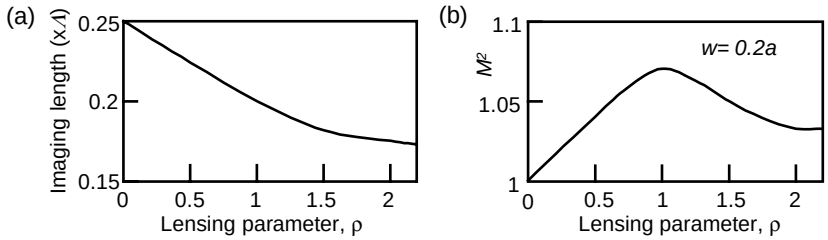

Fig. 7. Variation of (a) the $\Lambda/4$ imaging length and (b) the output M^2 factor at this length, as a function of the lensing parameter ρ

5. Conclusion

This paper has shown that self-imaging in multi-mode planar waveguides provides a powerful tool for the design of systems which combine free-space and waveguide propagation, for high average power solid-state lasers. Methods to evaluate the effects of misalignment, saturation and thermal lensing have been introduced. The techniques are particularly valuable for our current 150 W Nd:YAG waveguide device [3,9] which is 60 mm long, matching the $\Lambda/4$ imaging length after allowance for the thermal lens effect, as in Fig. 7. Current levels of pumping correspond to the lensing parameter ρ in the range 0.2 to 0.4. Recently, we have demonstrated single pass amplification of a gaussian beam [9] and have obtained a transverse M^2 of 1.14 for operation of the waveguide section as an oscillator in a mode-selective external cavity.

Acknowledgement

This work is supported by the UK Engineering and Physical Sciences Research Council.